Entropy **2013**, *15*, 2398-2414; doi:10.3390/e15062398

OPEN ACCESS

entropy

ISSN 1099-4300

www.mdpi.com/journal/entropy

Article

On the Use of Information Theory to Quantify Parameter Uncertainty in Groundwater Modeling

Alston Noronha [1] and Jejung Lee [2,*]

[1] Black and Veatch, 5750 Castle Creek Pkwy N Dr, Indianapolis, Indiana 46250, USA; E-Mail: alstonmn@yahoo.com

[2] Department of Geosciences, University of Missouri, Kansas City, 5100 Rockhill Road, Kansas City, Missouri, 64110, USA

* Author to whom correspondence should be addressed; E-Mail: leej@umkc.edu; Tel.: +1-816-235-6495; Fax: +1-816-235-5535.

Received: 16 February 2013; in revised form: 3 June 2013 / Accepted: 5 June 2013 / Published: 13 June 2013

Abstract: We applied information theory to quantify parameter uncertainty in a groundwater flow model. A number of parameters in groundwater modeling are often used with lack of knowledge of site conditions due to heterogeneity of hydrogeologic properties and limited access to complex geologic structures. The present Information Theory-based (ITb) approach is to adopt entropy as a measure of uncertainty at the most probable state of hydrogeologic conditions. The most probable conditions are those at which the groundwater model is optimized with respect to the uncertain parameters. An analytical solution to estimate parameter uncertainty is derived by maximizing the entropy subject to constraints imposed by observation data. MODFLOW-2000 is implemented to simulate the groundwater system and to optimize the unknown parameters. The ITb approach is demonstrated with a three-dimensional synthetic model application and a case study of the Kansas City Plant. Hydraulic heads are the observations and hydraulic conductivities are assumed to be the unknown parameters. The applications show that ITb is capable of identifying which inputs of a groundwater model are the most uncertain and what statistical information can be used for site exploration.

Keywords: information theory; groundwater modeling; parameter uncertainty

---

1. Introduction

Uncertainty of groundwater modeling has been one of the biggest challenges in hydrogeology for the last three decades. Many scientific efforts have been made to develop more comprehensive and computationally efficient models involving complex hydrogeologic processes. In spite of vigorous efforts of groundwater modeling, there are still limitations in the prediction of groundwater flow and hydrogeologic conditions with certainty. Groundwater modeling generally requires a large number of input parameters consisting of hydrogeologic parameters and numerical parameters. Hydrogeologic parameters such as hydraulic conductivity, storativity, and recharge rate are determined by various field tests and laboratory experiments. The inevitable limitations in determining such hydrogeologic parameters are: (1) the hydrogeologic structure is often too heterogeneous to be converted into simple discrete parameters in a model, (2) only a limited amount of data that is sparsely distributed over the site is available, and (3) measurement errors from poor equipment operation or human errors generate erroneous parameter values. Numerical parameters determine computational configurations such as grid size, boundary conditions, and time step. These parameters are generally determined by the user's subjective information and decision, which often produce non-uniqueness in obtaining solutions.

Inverse modeling, which is also called parameter optimization, is capable of managing the limitations mentioned above. It estimates unknown or uncertain parameters by minimizing errors between model outputs and observations. The model is said to be accurate if the difference between the model outputs and observations lies within acceptable limits (a predefined limit). One of the major concerns of inverse modeling is the non-uniqueness of the optimized parameters [1]. This non-uniqueness of inverse modeling makes it important to define the magnitude of the prediction uncertainty for the optimized parameters.

Papers [2] and [3] reviewed various optimization techniques and statistical methods for groundwater modeling. Among many uncertainty analysis techniques the first-order approximation method and the Monte Carlo simulation have been widely studied in groundwater modeling. The first-order approximation method is to approximate a non-linear groundwater model into a linear model using Taylor series expansion and calculate uncertainties of input parameters or output predictions [4,5]. The advantage of the first-order approximation method is fast computing time for high dimension and multivariate models. The linearity is, however, a major drawback especially when the model is highly non-linear. The Monte Carlo simulation is a stochastic method involving probabilistic distributions of inputs and outputs. The major advantage of the Monte Carlo method is that it estimates uncertainties of non-linear models based on the probabilistic information of inputs and/or outputs. The disadvantage is its expensive computing time especially for multidimensional non-linear models, but the fast performance of modern computers alleviates this concern and makes it more widely used in recent years [6,7].

The use of information theory in groundwater modeling has been very limited so far. The beginning of the information theory application was when Shannon's information theory [8] was incorporated into the principle of maximum entropy by Jaynes [9] for statistical mechanics. The basic concept of Jaynes' maximum entropy approach is that when making inferences based on incomplete information for given expectations (prior information) of a univariate or multivariate random function, the probability distribution must have the maximum entropy permitted by the available information expressed in the form of constraints [10]. The maximum entropy approach was applied to various geophysical problems such as seismic spectral analysis [11], seismic deconvolution [12], and earthquakes [13]. Singh [10]

reviewed the maximum entropy applications in the studies of hydrology and water resources. The use of maximum entropy in hydrology is somewhat limited to evaluate the efficiency of monitoring networks [14] such as a water quality network [15]. Woodbury and Ulrych [16] developed a different approach of entropy estimation called minimum relative entropy for groundwater models. In the minimum relative entropy, knowledge of moments is used as "data" rather than sample values. This method presumes knowledge of a prior probability distribution and produces the posterior probability distribution based on the information provided by new moments. Details of the minimum relative entropy are found in [16].

The goal of the present paper is to address applicability of information theory for the quantification of parameter uncertainty at the most probable state of hydrogeologic conditions in groundwater modeling. The groundwater flow modeling error from the parameter optimization is employed in a form of probability function to calculate the parameter uncertainty. The strength of the present Information Theory-based (ITb) approach is that it is applicable to any model and any inversion process as it was applied to a biocell model [17] and a basin model [18].

2. Methodology: Information Theory-Based Approach

The overall framework of ITb approach is shown in Figure 1. We adopted MODFLOW-2000 [19] as a groundwater model simulator. There are two types of parameters to be determined for the groundwater flow model. "Input parameters" are hydrogeologic parameters such as aquifer thickness, porosity, initial hydraulic heads, and pumping rates that are usually measured in the field. "Model parameters" are numerical parameters such as cell size, model dimension, number of layers, number of zones, convergence criteria, and number of time steps and stress periods. These model parameters are usually determined during the model conceptualization. When the groundwater model is fully conceptualized and set up in a numerical form, MODFLOW-2000 optimizes the uncertain input parameters and calibrates the model. When the model is fully optimized, a finite-difference approximation method [20] is conducted to calculate a Hessian matrix of ITb. The information theory formulation calculates statistics of uncertain input parameters such as standard deviation, covariance matrix, and correlation coefficient that can be used for statistical analysis to direct additional site exploration.

3. Information Theory Formulation

The information theory formulation is based on the entropy equation developed by [8]. Assume that the system involves a series of possible states of $\mathbf{x}$ and $\rho(\mathbf{x})$ is the probability when the state is $\mathbf{x}$. Each state of $\mathbf{x}$ is obtained considering a different set of parameters in a model, $\mathbf{x}=\{x_1, x_2, \ldots, x_n\}$ where x_i is an individual parameter of the model and n is the total number of parameters. The quantity $-\log\rho(\mathbf{x})$ quantifies how surprised one would be if the state is $\mathbf{x}$. For example, if $\rho(\mathbf{x})$ is small when the state is $\mathbf{x}$, one would be surprised. Likewise, one would be less surprised if $\rho(\mathbf{x})$ is large. In groundwater modeling, a state variable $\mathbf{x}$ is assumed to be continuous so that the probability $\rho(\mathbf{x})$ is a continuous function ranging from zero for an impossible state to one for a certain state. The expected surprise or entropy S is then given by:

$$S=-\int \rho(\mathbf{x})\ln\rho(\mathbf{x})\,d\mathbf{x} \tag{1}$$

Since S shows how surprised one would be by knowing the state of $\mathbf{x}$, S is a measure of the uncertainty associated with $\rho(\mathbf{x})$. If $\mathbf{x}$ is known, $\rho(\mathbf{x})$ is one and S becomes zero. If occurrence of $\mathbf{x}$ is equally likely, then S is maximum. Therefore, $\rho(\mathbf{x})$ is the probability that maximizes S constrained by the available data.

Figure 1. Flowchart of ITb approach using MODFLOW-2000.

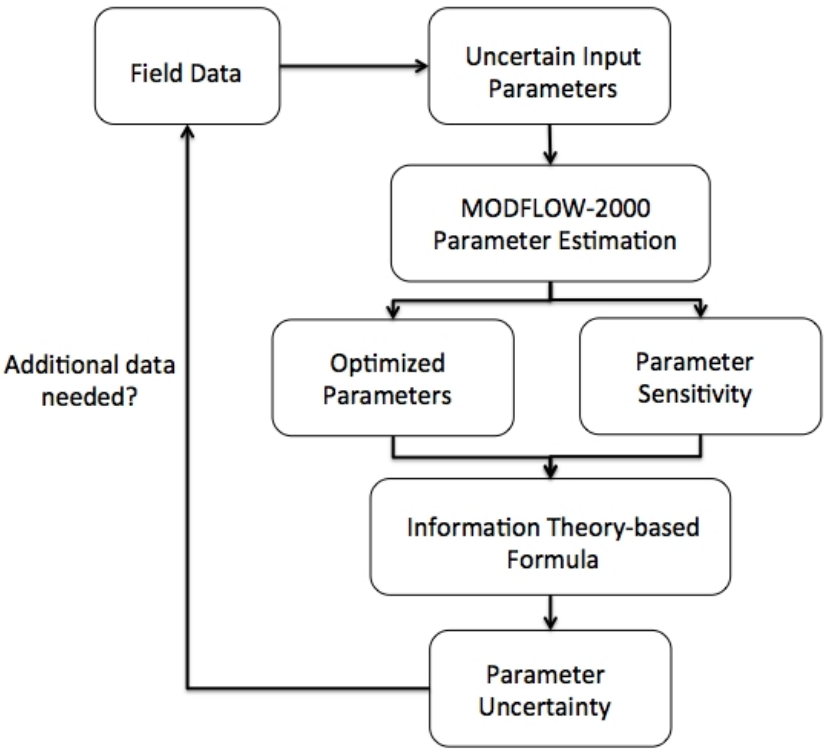

Two constraints are introduced to obtain unbiased probability $\rho(\mathbf{x})$. The first constraint is the normalization constraint:

$$\int \rho(\mathbf{x})d\mathbf{x} = 1 \tag{2}$$

This is the basic constraint stating that the sum of the probabilities of all possible states in a system should be equal to one. The second constraint is the error constraint associated with the error from available data. For example, if hydraulic heads constrain a ground flow model, the error function $E(\mathbf{x})$ becomes zero as the difference between observed heads and simulated heads goes to zero. Associating $E(\mathbf{x})$ with $\rho(\mathbf{x})$, the expected error E^* is given by:

$$E^* = \int \rho(\mathbf{x})E(\mathbf{x})d\mathbf{x} \tag{3}$$

In groundwater modeling, E^* can be the observation errors such as spurious fluctuations of head or conceptual model errors. To construct $\rho(\mathbf{x})$, S is constrained by Equations (2) and (3) using Lagrange's method [21]. The detailed mathematical calculation is described in the Appendix. The probability $\rho(\mathbf{x})$ for the most probable state of $\mathbf{x}$ is:

$$\rho(\mathbf{x}) = \prod_{i=1}^{N_P} \sqrt{\frac{N_p \lambda_i}{4\pi(E^* - E_{\min})}} \exp\left(-\frac{N_p \Delta\mathbf{x}^T H_{\mathbf{x}}[E(\mathbf{x})]\Delta\mathbf{x}}{4(E^* - E_{\min})} \right) \tag{4}$$

where N_p is the number of model parameters, $H_{\mathbf{x}}[E(\mathbf{x})]$ is the Hessian matrix for $E(\mathbf{x})$, λ_i is the eigenvalue of $H_{\mathbf{x}}[E(\mathbf{x})]$, $E_{\min}$ is the global minimum of $E(\mathbf{x})$, $\Delta\mathbf{x}$ is the perturbation vector on $\mathbf{x}$, and $\Delta\mathbf{x}^T$ is the transpose of $\Delta\mathbf{x}$.

Implementation of Equation (4) starts with parameter optimization. After the parameters of interest are optimized at $E_{\min}$, the Hessian matrix $H_{\mathbf{x}}[E(\mathbf{x})]$ and its eigenvalues are calculated around the optimized parameter $\mathbf{x}$ using a finite-difference approximation method [20]. For multivariate cases, the covariance of parameters can be obtained from the Hessian matrix. In the Gaussian domain, the multivariate probability density function is given as:

$$\rho(\mathbf{x}) = \frac{1}{(2\pi)^{N_P/2}\sqrt{\det C}} e^{-\frac{1}{2}(\mathbf{x}-\mathbf{x}_m)^T C^{-1}(\mathbf{x}-\mathbf{x}_m)} \tag{5}$$

where $\mathbf{x}_m$ is the mean vector; C is the covariance matrix of $\mathbf{x}$; and $\det C$ is the determinant of C [22]. As $\mathbf{x} \to \mathbf{x}_m$, the covariance C is obtained by:

$$C = \frac{2(E^* - E_{min})}{N_P} H_X^{-1}[E(\mathbf{x})] \tag{6}$$

where $H_X^{-1}[E(\mathrm{x})]$ is the inverse matrix of $H_{\mathbf{x}}[E(\mathbf{x})]$. Mathematically, E^* should be greater than E_{min} because the Hessian matrix should be positive-definite at a minimum. However, in practical usage, this condition may not be satisfied as E^* is dependent upon the data constraining the model. If the optimization goal is to have the minimum difference between E^* and E_{min}, the absolute difference between E^* and E_{min} can be used in Equation (4). Since Equation (4) is an analytic equation of $\rho(\mathbf{x})$, it is compatible with any optimization technique and any groundwater model.

We adopted a finite difference approximation method [20] to obtain second-order derivatives of functions for the Hessian matrix. For the diagonal elements of the Hessian matrix, centered difference approximation for a univariate function $f(x)$ was used:

$$f''(x) \simeq \frac{f(x+2\Delta x) - 2f(x+\Delta x) + f(x)}{\Delta x^2} \tag{7}$$

where $f''(x)$ is the second-derivative of $f(x)$ for a given small value of Δx. The off-diagonal elements of the Hessian matrix are in a form of bivariate function $f(x_1, x_2)$ and its second-order derivative function is:

$$f''(x_1, x_2) = \frac{f(x_1+\Delta x_1, x_2+\Delta x_2) - f(x_1+\Delta x_1) - f(x_2+\Delta x_2) + f(x_1, x_2)}{(\Delta x_1)(\Delta x_2)} \tag{8}$$

where $f''(x_1, x_2)$ is the second-derivative of $f(x_1, x_2)$ for given small values of Δx_1 and Δx_2 for variables of x_1 and x_2, respectively.

4. MODFLOW-2000

MODFLOW-2000 [19] is a three-dimensional finite difference model consisting of five processes: Global (GLO), Ground-Water Flow (GWF), Observation (OBS), Sensitivity (SEN), and Parameter-Estimation (PES) processes. The GLO process is to control overall program for four other processes, open files, and read global data such as space and time discretization into finite-difference grids. The GWF process is to solve groundwater flow equations including the formulation of the finite-difference

equations and data inputs and outputs. The OBS process compares model outputs with observed or measured quantities. Statistics produced by the OBS process and a post-processing program can be used to evaluate the accuracy of the model. The SEN process calculates sensitivities of hydraulic heads throughout the model with respect to specified input parameters. If the OBS process is active, observation sensitivities for the simulated head values are calculated using grid sensitivities. A modified Gauss-Newton nonlinear regression method is used in the PES process to calibrate input parameters in an iterative manner by minimizing the weighted least-squares objective function. In MODFLOW-2000, PES iterations are used to solve the nonlinear regression problems and these iterations begin with the starting input parameter values listed in the SEN process input file. A steady-state simulation calculates sensitivities only once for a single time step while a transient state simulation calculates hydraulic heads and their sensitivities at each stress period of time.

5. Implementation of ITb with MODFLOW-2000

The ITb is performed after the model is optimized by MODFLOW-2000. Implementing Equations (7) and (8) requires the head outputs from the optimized parameters and additional sets of head outputs by adding user-defined Δx to the optimized parameters. Equations (7) and (8) are then used to create the Hessian matrix that contains the approximate partial second derivatives of head with respect to the uncertain input parameters. Using the eigenvalues of the Hessian matrix Equation (6) calculates the covariance matrix, the standard deviation, and the correlation coefficients of the optimized input parameters. Since the optimized parameters are linked to explicit features over a specific area in a study site, the area associated with the most uncertain parameter is the area that needs further site exploration. In this manner the site exploration becomes efficient and would be cost-effective to save time, labor, and resources.

6. Synthetic Model Application

We adopted an example case cited in [19] to verify validity of the ITb approach. The setup for this synthetic model is shown in Figure 2. The system consists of two confined aquifers, each 50 m thick. The upper aquifer is labeled as Aquifer 1 and the lower one as Aquifer 2. A 10 m thick confining unit separates the two confined aquifers. A river flows west of this system and is hydraulically connected to Aquifer 1. To simulate the river, the entire west boundary is treated as a head-dependent boundary fixed to the constant value of 100 m. Towards the east is an adjoining hillside, which is a major contribution to the recharge of the system. This recharge is assumed to be known and hydraulically connected to both the Aquifers 1 and 2. A constant head boundary of 100 m is set along the east side of the system representing a flow divide. Areal recharge to Aquifer 1 is divided into two equal zones. Zone 1 is closer to the river and Zone 2 is farther away from the river. No flow boundaries are set up on the north and south sides. Wells are present in the studied area as shown in Figure 2b. There is one well, centrally located, that is assumed to pump water with the same flow rate from both the aquifers. The model has an area of 18,000 m by 18,000 m and is discretized into 1,000 m by 1,000 m sized squares so that the grid has 18 rows and 18 columns. For the finite-difference method, time discretization is specified to simulate the model for a steady state period followed by a transient state period. The steady state period has no pumping and is simulated with one stress period having one time step. The transient period has a constant pumping rate and is simulated with four stress periods

having one time step. The first three stress periods are 1, 3, and 6 days long, and each has one time step; the fourth is 272.8 days long and has 9 time steps, and each time-step length is 1.2 times the length of the previous time-step length [19]. Other parameters and their values are listed in Table 1 and model input files are provided in [19].

Figure 2. The synthetic model setup. (**a**) The original schematic setup in Hill *et al.* [19]. (**b**) Plan view of the synthetic model setup.

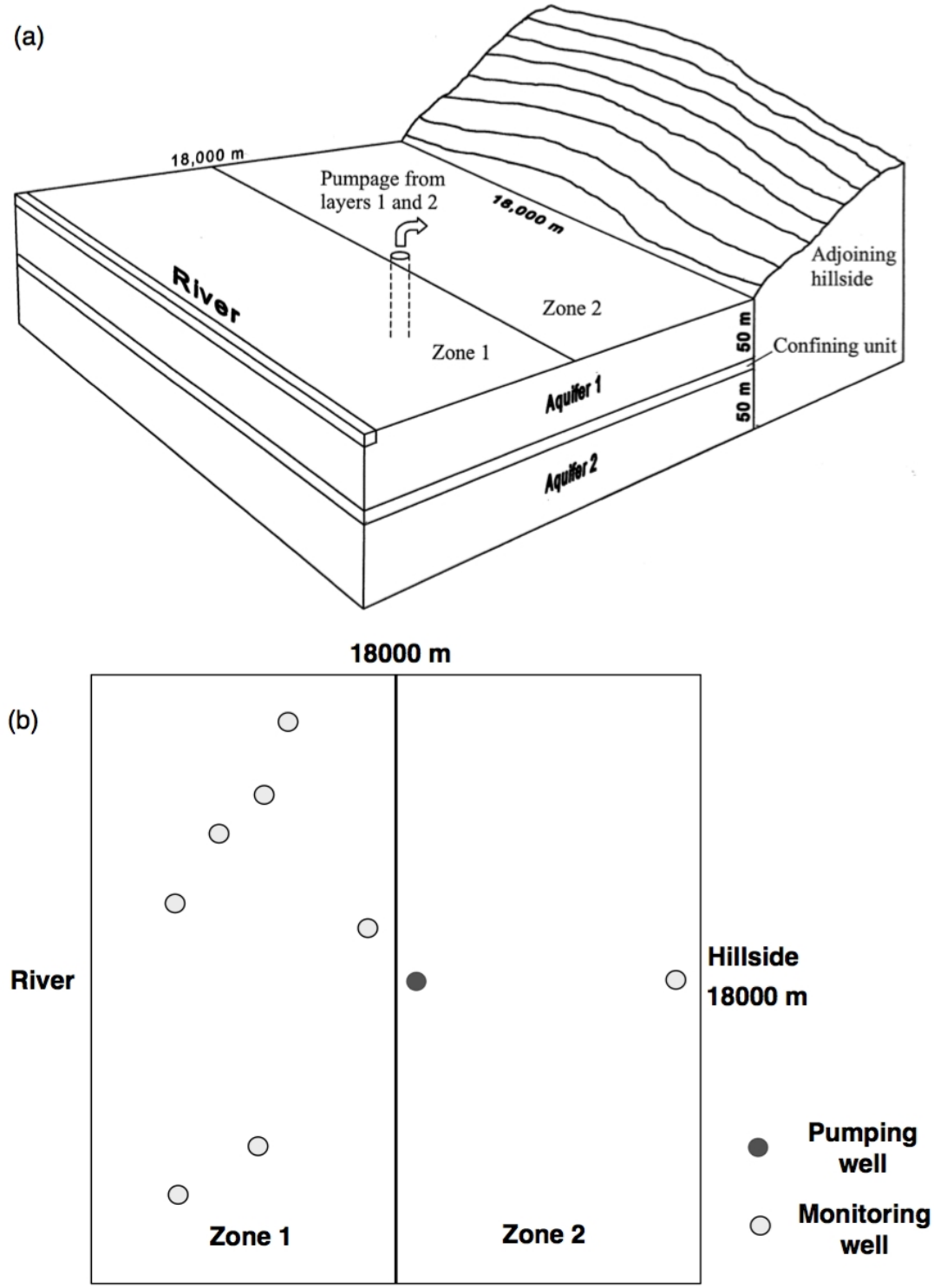

Table 1. Input parameters for the synthetic model.

Parameter	Value
Recharge in Zone 1, RCH_1	0.63 m/yr
Recharge in Zone 2, RCH_2	0.32 m/yr
Storage coefficient of Aquifer 1, SS_1	1.3×10^{-3}
Storage coefficient of Aquifer 2, SS_2	2.0×10^{-4}
Vertical hydraulic conductivity of confining layer	1.0×10^{-7} m/s
Hydraulic conductivity of riverbed	1.2×10^{-3} m/s
Hydraulic conductivity of Aquifer 1, HK1	3.0×10^{-4} m/s
Hydraulic conductivity of Aquifer 2, HK2	4.0×10^{-5} m/s
Pumping rate in each layer 1 and 2	1.10 m^3/s
Hydraulic head of river	100 m

The parameters in Table 1 are considered as uncertain parameters in [19]. In the present application of ITb, the hydraulic conductivity of Aquifer 1, HK1 and that of Aquifer 2, HK2 are the two target parameters to be optimized while other parameter values are fixed. The observed hydraulic heads are obtained from the sampling wells shown in Figure 2. The starting values, true values and optimized values of HK1 and HK2 are listed in Table 2. The minimum error E_{min}, which is the sum of squared, weighted residual of MODFLOW-2000 at the optimized state, was 43.37 (unitless). After running MODFLOW-2000, we applied the ITb to generate the Hessian matrix and its eigenvalues by perturbing the hydraulic conductivities for the hydraulic heads. The results of the ITb calculation are shown in Table 3. The value of the expected error, E^* is assumed to be 100 (unitless). Table 3 shows that the standard deviation of HK1 is almost ten times greater than that of HK2, which may imply that HK1 is more uncertain than HK2. However, this may not be true as the optimized values of HK1 and HK2 are also an order of magnitude apart. To avoid the scale difference the coefficient of variation was calculated for each parameter as listed in Table 3. The coefficient of variation shows that HK1 is still more uncertain than HK2. The correlation coefficient is −0.76 suggesting that HK1 and HK2 are closely related in opposite direction of change, so that an increase in one will result in a decrease in the other and vice versa. Figure 3 shows the bivariate probability density function (PDF) and univariate PDFs for HK1 and HK2 using the variance in Equation (6). The univariate PDFs indicate that the true values of HK1 and HK2 are located within the range of standard deviation around the optimized values. This proves that for the given head observations, the optimization process of MODFLOW-2000 is successful in estimating HK1 and HK2. Figure 4 shows the change of parameter uncertainty with respect to the different expected errors. If the expected error is much greater or smaller than the global minimum, then the uncertainty increases. The bars represent the standard deviation of HK1. It is clearly shown that as the expected error increases, there is a subsequent increase of the parameter uncertainty.

Table 2. Parameter values after optimization process of MODFLOW-2000.

Parameter	*True Value*	*Starting Value*	Optimized Value
HK1 (m/s)	4.0×10^{-4}	3.0×10^{-4}	4.26×10^{-4}
HK2 (m/s)	4.4×10^{-5}	4.0×10^{-5}	4.82×10^{-5}

Table 3. Statistical outputs of the synthetic model.

Parameter	Standard Deviation (m/s)	Coefficient of Variation (Unitless)
HK1	5.25×10^{-5}	10.23×10^{-2}
HK2	4.76×10^{-6}	9.88×10^{-2}

Figure 3. The bivariate probability density function (PDF) and univariate PDFs for HK1. and HK2.

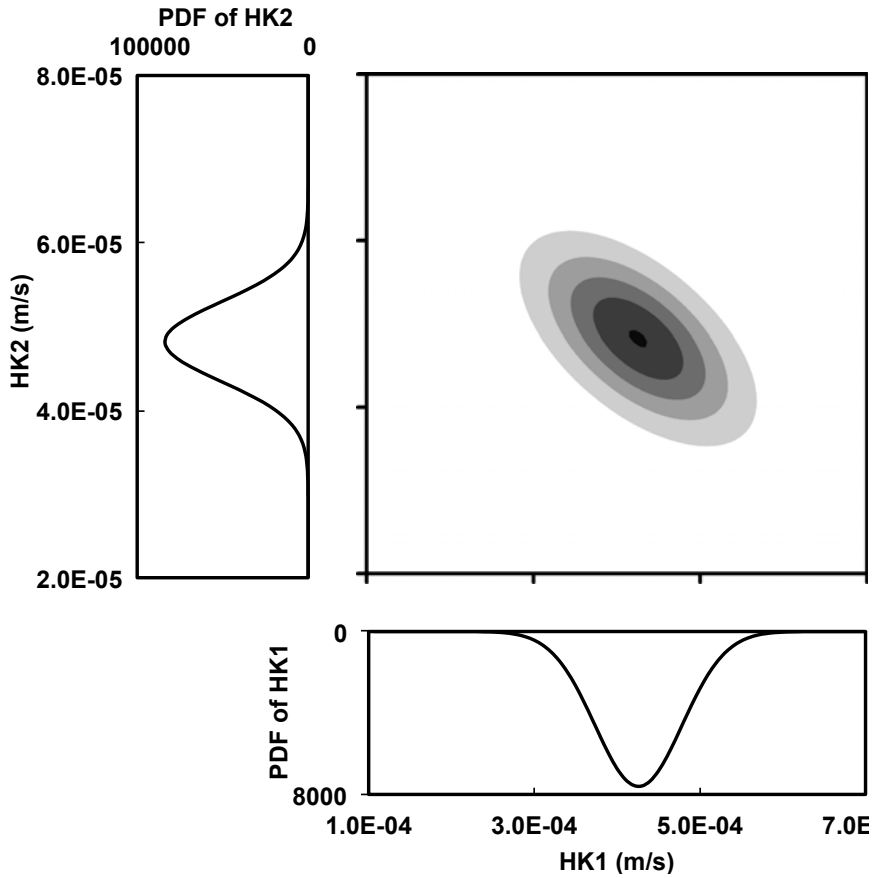

Figure 4. Parameter uncertainty of HK1 for the expected error E*. The bars indicate the standard deviation of HK1.

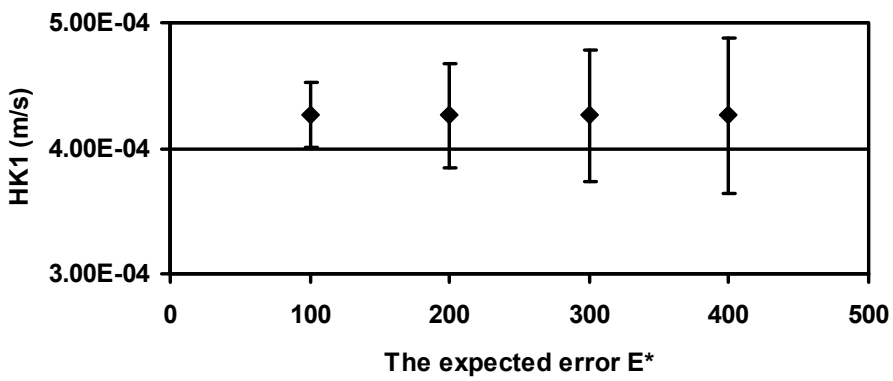

7. Case Study: Kansas City Plant

The Kansas City Plant (KCP) is located 12 miles south of downtown Kansas City, Missouri. It was established in 1942 and occupies approximately 141 acres of the 300-acre Bannister Federal complex.

The KCP is responsible for production and procurement of non-nuclear components for nuclear weapons. The KCP does not perform any onsite waste disposal. Onsite sanitization is mainly for non-hazardous classified wastes. The hazardous wastes are sent offsite for treatment or disposal. The waste management operations at the plant mainly consist of storing these hazardous wastes until they are taken offsite. In addition to hazardous wastes, some low-level radioactive wastes are also generated. For national security reasons, some wastes are classified. Selective recycling and industrial wastewater pretreatment are the main treatment operations at the KCP [23].

From the 1940s to the 1960s, a part of the northeast area (NEA) was used as a dumping site for waste from the KCP, resulting in extensive soil and groundwater contamination. Additional contamination from the release of polychlorinated biphenyl (PCB) and a man-made chemical, which was banned from U.S. manufacturing in 1979, continued through the early 1970s [23]. The immediate concern was the contaminant plume getting into the Blue River (Figure 5). The contaminant plume consisted of volatile organic compounds including trichloroethylene, 1,2-dichloroethylene, and vinyl chloride. To prevent migration of the contaminant to the Blue River, an interceptor trench was installed in 1990 and operated until 1998 to catch the plume. After extensive site investigation in 1998, a passive iron wall permeable reactive barrier (PRB) was installed to replace the interceptor trench. This passive iron wall was not successful as the contaminant bypassed the southern end of the wall. The groundwater flow simulation predicted that containment of the contaminant would require pumping rates in excess of 30 gallons per minute (gpm). The existing interceptor trench tried to contain the contaminant by pumping at a rate of 6 gpm, hence the modeling design was discarded and further hydrological analysis of the NEA groundwater flow system was made [23]. To characterize the groundwater flow system, [23] collected data from 28 newly installed temporary wells and the existing monitoring wells, 12 stilling wells, four mini-piezometers, and a weir. Recharge from the cattail drainage was found to cause groundwater mounding, which deflected the plume to the east soon after entering the lower NEA (Figure 5). This mound was considered to be a consistent hydrologic feature because of the frequent storm events in Kansas City. The plume in the vicinity of the iron wall was more than 60 m wide.

For the ITb application we divided the area of study into 50 by 50 cells that are 4.42 m by 4.16 m giving us an area of approximately 221 m in the east-west direction and 208 m in the north-south direction. The geology consists of alluvial sediments overlaying impervious shale. The alluvial aquifer in the lower NEA consists of a 4.57 to 7.62 m thick upper clayey-silt layer underlain by a 0.30 to 1.52 m thick basal gravel layer. The contrast of hydraulic conductivities in these two layers made the potentiometric surface of the more permeable basal gravel layer 0.3 m to 0.6 m lower than the potentiometric surface in the less permeable clayey-silt, creating a downward hydraulic gradient. For modeling purposes we considered the clayey-silt layer and the basal gravel layer to be of average thickness 5.49 m and 0.91 m, respectively, with average hydraulic conductivities of 0.23 m/day and 10.36 m/day, respectively. The dimensions of the interceptor trench were 4.57 m wide, 65.53 m long and 9.14 m deep. The iron wall PRB was designed such that it was 0.6 m wide in the 5.5 m deep upper clayey-silt layer and 1.83 m wide in the basal gravel layer, with a length of 39.62 m and hydraulic conductivity ranging from 91.44 to 152.4 m/day.

Figure 5. The hydraulic conductivity distribution for the KCP site (modified from [23]). Each zone of hydraulic conductivity is defined with a closed boundary and different color. (**a**) The lower basal gravel layer. (**b**) The upper clayey silt layer.

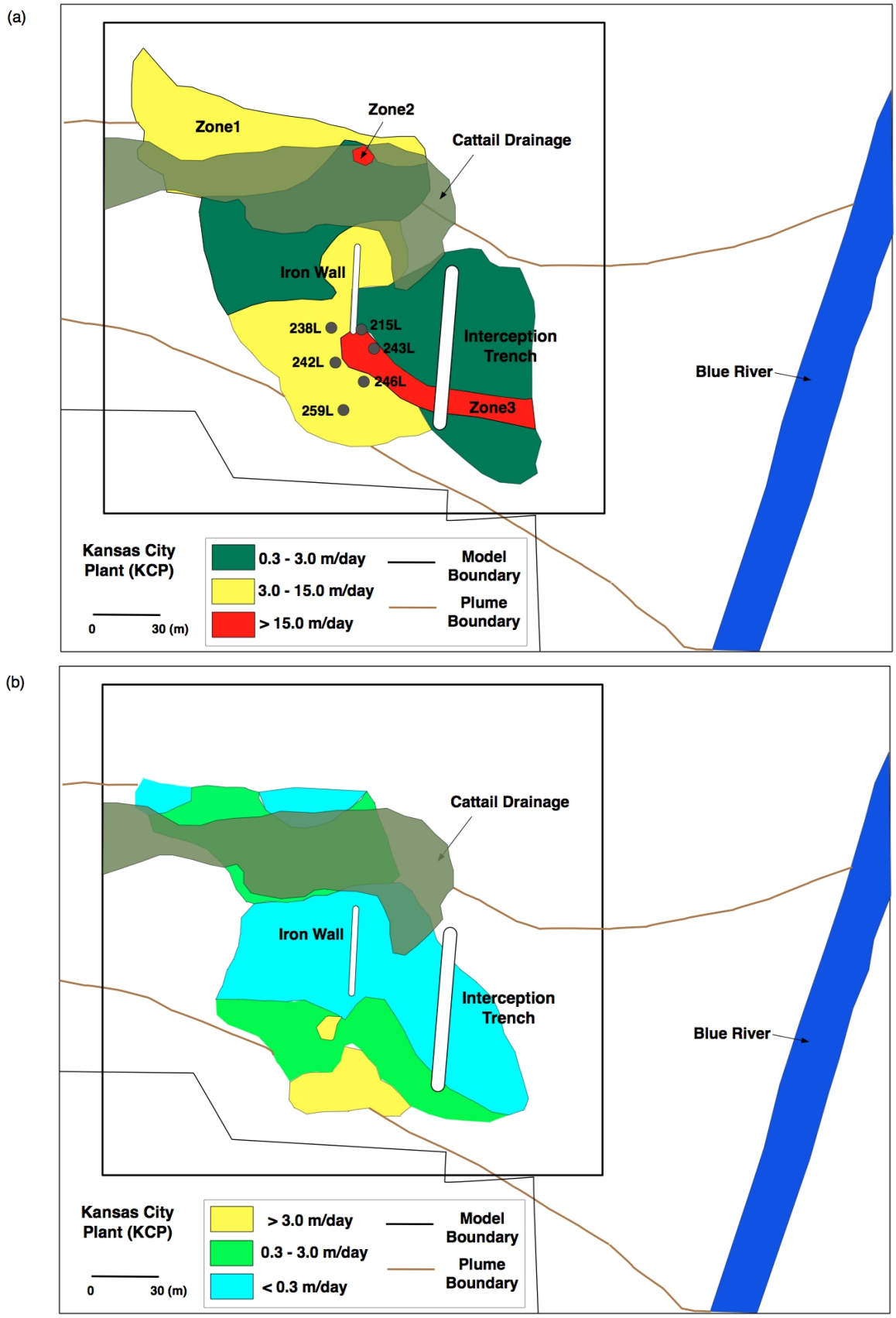

In the KCP model, we adopted head observations from the 26 wells located in the model domain and used them for a steady state simulation; hence the stress period for all observations was 1. The hydraulic conductivity values were obtained from [23] for the clayey-silt layer and the basal gravel layer. The hydraulic conductivity values from the wells in each zone were averaged and assigned as a zonal hydraulic conductivity for that zone. The SEN file had the hydraulic conductivities of the 18 zones in the model. The clayey-silt and the basal gravel layers had seven different hydraulic conductivity zones each (Figure 5). The remaining four zones were used for the layer of peat or humus, the fill layer, and the areas around the clayey-silt and the basal gravel layers. The model was set up with no flow boundaries on the north and south boundaries. The west boundary had a constant head boundary while the east boundary had no flow boundary. We assumed the vertical hydraulic conductivity to be 1/20 times that in the horizontal direction. The head change and residual convergence criteria were both taken as 1.0E-5 and no damping was set in the model.

The KCP case study [23] listed the observed minimum and maximum hydraulic conductivities of all the wells in both the upper clayey-silt layer and the lower basal gravel layer. Among them the six wells having the largest difference of hydraulic conductivities are listed in Table 4 and located in Figure 5a. The well numbers with "L" stand for the lower basal gravel layer. Note that the difference between minimum and maximum hydraulic conductivities is up to nearly ten times that of the minimum value. During the PRB design process the averages of such highly variable hydraulic conductivities were adopted [23]. Interestingly all the six wells are located south of the iron wall of PRB where the contaminant plume bypassed.

Table 4. Pumping test results at six selected wells in Figure 5.

Well Number	Minimum Hydraulic Conductivity (m/day)	Maximum Hydraulic Conductivity (m/day)	Average Hydraulic Conductivity (m/day)
215L	30.96	149.81	89.88
238L	23.86	238.59	131.23
242L	24.91	249.06	136.98
243L	21.88	54.71	38.30
246L	20.19	201.89	111.04
259L	23.89	119.45	71.67

For the ITb application, we targeted three zones having different hydraulic conductivities. We included the zone where the plume bypassed the PRB and also two other zones around cattail drainage having recharge of water that deflected the groundwater flow towards east and south. We limited the number of zones to just three because the complexity and computational time increases with addition of more zones. All three zones were located in the lower basal gravel layer as shown in Figure 5(a). We named those as Zones 1, 2, and 3, respectively. The initial values for Zones 1, 2, and 3 were optimized using MODFLOW-2000 to give the best representation of model-to-site configuration. The minimum error from the MODFLOW-2000 was E_{min} = 32.37 (unitless). The standard deviation of the three parameters and their correlation coefficients along with initial and optimized hydraulic conductivities are listed in Table 5. We assumed the expected error $E^*$to be 40 (unitless). It is shown that Zone 3 is the most uncertain of the three. As discussed in [23], this zone has three to ten times

higher hydraulic conductivity compared to the one used in the PRB design. The correlation coefficients show that there is almost no correlation between Zones 1 and 3, and Zones 2 and 3, while Zones 1 and 2 are negatively correlated, meaning that an increase of hydraulic conductivity in Zone 1 would lead to a decrease of hydraulic conductivity in Zone 2 and vice versa. If additional site exploration is required, Zone 3 would be the first area to be investigated since it has the most uncertain hydraulic conductivity estimation.

Table 5. Optimized hydraulic conductivities and standard deviations for three zones of the Kansas City Plant (KCP) model.

Zone	Initial Hydraulic Conductivity (m/day)	Optimized Hydraulic Conductivity (m/day)	Standard Deviation (m/day)
1	9.22	13.02	129.33
2	17.11	31.15	30.89
3	26.44	32.81	155.25

Correlation Coefficient between Zone 1 and Zone 2 = -0.51E-00; Correlation Coefficient between Zone 1 and Zone 3 = −9.85E-02; Correlation Coefficient between Zone 2 and Zone 3 = -9.85E-02.

8. Conclusions

We developed an ITb formulation to quantify uncertainty of optimized parameters for a groundwater model. In developing ITb formulation, the normalization constraint and the error constraint are imposed because they are the most objective information that is statistically reliable during a modeling process. The expected error is generally defined by conceptual model errors, measurement errors such as spurious fluctuations of head or instrumentation errors. If the parameters are optimized at the global minimum of modeling error and the global minimum is close to the expected error, the model result is likely to have low uncertainty because the size of expected error is similar with the global minimum of the model error. The ITb approach is capable of identifying which inputs of a groundwater model are the most uncertain and which information can be used for additional site exploration.

Acknowledgements

The Faculty Research Grant from the University of Missouri—Kansas City, funded the present study. The authors would like to thank the anonymous reviewers for their careful review and constructive comments.

Conflict of Interest

The authors declare no conflict of interest.

Appendix A—Information Theory Formulation [18]

We refer to [18] for better understanding of ITb formulation for readers. The entropy, S is given by:

$$S = -\int \rho(\mathbf{x}) \ln \rho(\mathbf{x}) d\mathbf{x} \tag{A1}$$

Two constraints are introduced to obtain the probability $\rho(\mathbf{x})$. The first constraint is the normalization constraint:

$$\int \rho(\mathbf{x}) d\mathbf{x} = 1 \tag{A2}$$

The second constraint is the misfit constraint associated with the error from available data. For the misfit function, $E(\mathbf{x})$, the "expected" misfit, E^* is given by:

$$E^* = \int \rho(\mathbf{x}) E(\mathbf{x}) d\mathbf{x} \tag{A3}$$

To construct $\rho(\mathbf{x})$, the entropy S is imposed by the constraints in Equations (A2) and (A3) using Lagrange's method [21]:

$$\tilde{S} = S - \alpha\left(\int \rho(\mathbf{x}) d\mathbf{x} - 1\right) - \beta\left(\int \rho(\mathbf{x}) E(\mathbf{x}) d\mathbf{x} - E^*\right) \tag{A4}$$

where α and β are the Lagrange multipliers. Maximization of $\tilde{S}$ with respect to $\rho(\mathbf{x})$ yields:

$$\frac{\delta \tilde{S}}{\delta \rho} = \int [-\ln \rho(\mathbf{x}) - (\alpha + 1) - \beta E(\mathbf{x})] d\mathbf{x} = 0 \tag{A5}$$

therefore:

$$-\ln \rho(\mathbf{x}) - (\alpha + 1) - \beta E(\mathbf{x}) = 0 \tag{A6}$$

For practical reasons, and to make the evaluation of the probability density feasible, we expand $\ln \rho(\mathbf{x})$ around the most probable state $\mathbf{x}_m$ of $\mathbf{x}$. The most probable state, $\mathbf{x}_m$ is obtained when the global minimum of $E(\mathbf{x})$ is reached. The most probable state, $\mathbf{x}_m$ also maximizes the probability density because $\ln \rho(\mathbf{x})$ is a monotonic function of ρ. Taylor expansion of $\ln \rho(\mathbf{x})$ around $\mathbf{x}_m$ gives:

$$\ln \rho(\mathbf{x}) = \ln \rho(\mathbf{x}_m) + \Delta\mathbf{x}^T \nabla_{\mathbf{x}} \ln \rho(\mathbf{x}) + \frac{1}{2} \Delta\mathbf{x}^T H_{\mathbf{x}}[\ln \rho(\mathbf{x})] \Delta\mathbf{x} + \cdots \tag{A7}$$

where $H_{\mathbf{x}}[\ln \rho(\mathbf{x})]$ is the Hessian matrix for $\ln \rho(\mathbf{x})$ with respect to $\mathbf{x}$ evaluated at $\mathbf{x}=\mathbf{x_m}$, $\Delta\mathbf{x}$ is the perturbation vector $\mathbf{x} - \mathbf{x}_m$, and $\Delta\mathbf{x}^T$ is the transpose of $\Delta\mathbf{x}$. The latter approximation is valid when we have a narrow probability distribution around $\mathbf{x}_m$, where the quadratic term is the dominant factor. The linear term is dropped since, by construction, the gradient of the probability density at its maximum is equal to zero. For a multi-modal probability distribution, when one of the maxima is larger than the others, it is legitimate to ignore the latter. Although a complete description of the probability could be obtained using few parameters (i.e., averages and variances), the idea of best estimate and confidence intervals would be irrelevant when the multimodal probability density has comparable maxima. From Equation (A6), the Hessian matrix in Equation (A7) becomes:

$$H_{\mathbf{x}}[\ln \rho(\mathbf{x})] = -\beta H_{\mathbf{x}}[E(\mathbf{x})] \tag{A8}$$

The quadratic approximation of the probability density is then given by:

$$\ln \rho(\mathbf{x}_m) = -(\alpha + 1) - \beta E_{\min} \tag{A9}$$

$$\ln \rho(\mathbf{x}) = \ln \rho(\mathbf{x}_m) - \frac{1}{2} \beta \Delta\mathbf{x}^T H_{\mathbf{x}}[E(\mathbf{x})] \Delta\mathbf{x} \tag{A10}$$

The probability function of $\rho(\mathbf{x})$ is rewritten as:

$$\rho(\mathbf{x}) = \rho(\mathbf{x}_m)\exp\left(-\frac{\beta\Delta\mathbf{x}^T H_{\mathbf{x}}[E(\mathbf{x})]\Delta\mathbf{x}}{2}\right) \tag{A11}$$

where:

$$\rho(\mathbf{x}_m) = \exp\left(-(\alpha+1) - \beta E_{\min}\right) \tag{A12}$$

To evaluate the multidimensional integrals required to calculate the constraints (A2) and (A3), we utilize the spectral decomposition of the Hessian matrix, $H_{\mathbf{x}}[E(\mathbf{x})]$, which is given by:

$$H_{\mathbf{x}}[E(\mathbf{x})] = G^T \lambda G \tag{A13}$$

where G is the eigenvector matrix and λ is a diagonal matrix whose diagonal entries are the eigenvalues of the Hessian matrix. We assume that the Hessian matrix of the misfit function is positive definite around $\mathbf{x}_m$. Such an assumption makes it possible to evaluate the quadratic integration analytically. For a multivariate case, the multivariate probability density function is given as:

$$\rho(\mathbf{x}) = \frac{1}{(2\pi)^{N_P/2}\sqrt{\det C}} e^{-\frac{1}{2}(\mathbf{x}-\mathbf{x}_m)^T C^{-1}(\mathbf{x}-\mathbf{x}_m)} \tag{A14}$$

where N_p is the number of model parameters; $\mathbf{x}_m$ is the mean vector; C is the covariance matrix of $\mathbf{x}$; and $\det C$ is the determination of C. As $\mathbf{x} \to \mathbf{x}_m$, the covariance C is obtained by:

$$C = \frac{1}{\beta} H^{-1}[E(\mathbf{x})] \tag{A15}$$

which satisfies:

$$\det\ C = 1 \Big/ \beta^{N_P} \prod_{i=1}^{N_P} \lambda_i \tag{A16}$$

By doing so, we arrive at an expression for the Lagrange multipliers α and β in terms of the eigenvalues of the Hessian matrix of the misfit function. These expressions are given by:

$$\alpha = \ln\left(\prod_{i=1}^{N_P}\sqrt{\frac{\beta\lambda_i}{2\pi}}\right) - 1 \tag{A17}$$

and:

$$\beta = \frac{N_P}{2(E^* - E_{\min})} \tag{A18}$$

where λ_i is the eigenvalue of $H_{\mathbf{x}}[E(\mathbf{x})]$, and $E_{\min}$ is the global minimum of $E(\mathbf{x})$.

By applying Equations (A17) and (A18) to Equation (A11), the probability distribution $\rho(\mathbf{x})$ around the most probable state of $\mathbf{x}$ is written as:

$$\rho(\mathbf{x}) = \prod_{i=1}^{N_P}\sqrt{\frac{N_p\lambda_i}{4\pi(E^* - E_{\min})}}\exp\left(-\frac{N_p\Delta\mathbf{x}^T H_{\mathbf{x}}[E(\mathbf{x})]\Delta\mathbf{x}}{4(E^* - E_{\min})}\right) \tag{A19}$$

In the ITb approach, Equation (A12) is calculated after parameter optimization. If the parameter of interest is optimized as $\mathbf{x}$ at $E_{\min}$, the Hessian matrix, $H_{\mathbf{x}}[E(\mathbf{x})]$ and its eigen values, λ_i are calculated around the optimized value, $\mathbf{x}$. Any optimization technique is compatible with this equation.

References

1. Abbaspour, K.C.; Johnson, C.A.; van Genuchten, M. Th. Estimating uncertainty flow and transport parameters using a sequential uncertainty fitting procedure. *Vadose. Zone J.* **2004**, *3*, 1340–1352.
2. McLaughlin, D.; Townley, L.R. A reassessment of the groundwater inverse problem. *Wat. Resour. Res.* **1996**, *32*, 1131–1161.
3. Hill, M.C. Methods and guidelines for effective model calibration. *US Geological Survey Water-Resources Investigation Report 98–4005*; 1998.
4. Kitanidis, P.K. *Introduction to Geostatistics.: Applications in Hydrogeology*; Cambridge University Press: Cambridge, England,1997.
5. Dettinger, M.D.; Wilson, J.L. First order analysis of uncertainty in numerical models of groundwater flow Part 1: Mathematical development. *Water Resour. Res*. **1981**, *17*, 149–161.
6. Blasone, R.-S.; Vrugt, J.A.; Madsen, H.; Rosbierg, D.; Robinson, B.A.; Zyvoloski, G.A. Generalized likelihood uncertainty estimation (GLUE) using adaptive Markov Chain Monte Carlo sampling. *Adv. Water Resour.* **2008**, *31*, 630–648.
7. Yoon, H.; Hart, D.B.; McKenna, S.A. Parameter estimation and predictive uncertainty in stochastic inverse modeling of groundwater flow: Comparing null-space Monte Carlo and multiple starting point methods. *Water Resour. Res.* **2013**, doi:10.1002/wrcr.20064.
8. Shannon, C.E. A mathematical theory of communication. *Bell. Syst. Tech. J*. **1948**, *27*, 379–423.
9. Jaynes, E.T. Information theory and statistical mechanics. *Phy. Rev*. **1957**, *106*, 620–630.
10. Singh, V.P. The use of entropy in hydrology and water resources. *Hydrol. Process.* **1997**, *11*, 587–626.
11. Haykin, S. *Nonlinear Methods of Spectral Analysis*, 2nd ed.; Springer Verlag: Berlin/Heidelberg, Germany, 1983.
12. Robinson, E.A.; Trietel, S. *Geophysical Signal. Analysis*; Prentice Hall: Upper Saddle River, NJ, USA, 1980.
13. Rietsch, E. The maximum entropy approach to the inversion of one-dimensional seismograms. *Geop. Prospecting*. **1988**, *36*, 365–382.
14. Lee, Y.-M.; Ellis, J.H. On the equivalence of kriging and maximum entropy estimators, *Math. Geol*. **1997**, *29*, 131–151.
15. Mogheir, Y.; Singh, V.P. Application of information theory to groundwater quality monitoring networks. *Water Resour. Manage*. **2002**, *16*, 37–49.
16. Woodbury, A.D.; Ulrych, T.J. Minimum relative entropy and probabilistic inversion in groundwater hydrology. *Stochastic Hydrol. Hydraulics*. **1998**, *12*, 317–358.
17. Sayyed-Ahmad, A.; Tuncay, K.; Ortoleva, P. Toward automated cell model development through Information theory. *J. Phy. Chem. A*. **2003**, *107*, 10554–10565.
18. Lee, J.; Sayyed-Ahmad, A.; Sheen, D.-H. Basin model inversion using information theory and seismic data. *Geophysics* **2007**, *72*, R99–R108.

19. Hill, M.C.; Banta, E.R.; Harbaugh, A.W.; Anderman, E.R. *MODFLOW-2000, The U.S. Geological Survey Modular Ground-Water Model.—User Guide to the Observation, Sensitivity, and Parameter-Estimation Processes and Three Post-Processing Programs*; US Geological Survey Open-File Report 00–184, 2000.
20. Eberly, D. Derivative Approximation by Finite Differences. *Magic Software, Inc.* Available online: http://www.geometrictools.com/ (accessed on 21 January 2003).
21. Bertsekas, D. *Constrained Optimization and Lagrange Multiplier Methods*; Academic Press: Waltham, MA, USA, 1996.
22. Mardia, K.V.; Kent, J.T.; Bibby, J.M. *Multivariate Analysis*; Academic Press: Waltham, MA, USA, 1997.
23. Department of Energy. *Lower Northeast Area Characterization and Iron Wall Evaluation Report*; U.S. Department of Energy, Kansas City Area Office: Kansas City, MO, USA, 2000.

© 2013 by the authors; licensee MDPI, Basel, Switzerland. This article is an open access article distributed under the terms and conditions of the Creative Commons Attribution license (http://creativecommons.org/licenses/by/3.0/).